33rd Annual International Conference of the IEEE EMBS
Boston, Massachusetts USA, August 30 - September 3, 2011

# *In vivo* Dynamic Imaging, *in silico* Modeling and Global Sensitivity Analysis for the Study and the Diagnosis of Epithelial Neoplasia

George Papoutsoglou, Antigoni Anastasopoulou, George Stavrakakis, Pat Soutter and Costas Balas, *Member*, *IEEE*

*Abstract*— **We present a method for detecting and studying neoplasia-specific functional and structural features through the combination of *in vivo* dynamic imaging, *in silico* modeling and global sensitivity analysis. We particularly present the case of cervical epithelium interacting with acetic acid solution, which is employed as an optical biomarker. The *in vivo* measured dynamic scattering characteristics are strongly correlated with the output of the biomarker's pharmacokinetic model that we have developed. Model global sensitivity analysis has shown that the measured/modeled bio-optical processes can be used for probing, *in vivo*, the number of neoplastic layers, the extracellular pH, the intracellular buffering efficiency and the size of the extracellular space.**

## I. Introduction

PHARMACOKINETC modeling of the uptake kinetics of optical biomarkers has been proven to be an indispensible tool for analyzing poly-parametric biological systems. Biology-inspired and physiology-based pharmacokinetic models have been extensively utilized in the design of *in vitro* experiments and in the analysis of system's responses to optical and chemical excitations [1],[2]. The majority of related work has been directed towards experiments targeting mainly the identification of cellular and/or subcellular processes associated with biosignaling, tumor growth etc. [3],[4].

Optical biomarkers have also been used as contrast agents for assisting the localization of abnormalities and for guiding biopsy sampling. Attempting to improve the diagnostic performance of the relevant *in vivo* diagnostic tests, Balas et al. developed a method and device for measuring and mapping the dynamic optical signals, generated during the biomarker-tissue interaction [5]-[7]. Particularly, by employing acetic acid (AA) dilute solution as a biomarker, the method was applied for the *in vivo*, non-invasive detection, identification and mapping of epithelial neoplasias of cervix, larynx and skin [8],[9]. In two large clinical trials, conducted in Europe and enrolling hundreds of patients, the method was proven to be very efficient, demonstrating an improvement of more than 63% in the diagnostic sensitivity over established methods [10],[11]. These findings indicate that the method has an evident clinical potential in non-invasive diagnosis of epithelial neoplasia. However, empirical/phenomenological comparison of dynamic optical data with histological results is not informative on the actual functional and structural alterations that are associated with the neoplasia growth. Assessment of all these biological factors can, in principle, be achieved through the combination of the *in vivo* measurement and mapping of the generated dynamic scattering signals and the modeling of the biomarker pharmacokinetics. To this end, we have identified a long list of biological parameters that are determining the AA pharmacokinetics and are correlated with the neoplasia growth [12]. A very important step forward is to elucidate whether these parameters can be probed through the macroscopically measured dynamic optical signals and particularly to identify a subset of these parameters, which are the most influential to the signals' line shapes. This is very essential since valuable knowledge will be gained on how functional and structural biological factors are independently or in combination altering during the neoplasia growth. This would be proved very useful in the better understanding of the biophysical mechanisms involved in neoplasia growth, by examining live epithelial tissue. Apart from that, the *in vivo* assessment of the structural and particularly the functional status of the tissue is expected to provide additional and valuable diagnostic information. This is because, in current practices, diagnosis and grading is based on the histological assessment of the structural changes, solely, in dead tissue biopsy samples. To stress this point further it is worth emphasizing that there is no established method for assessing functional characteristics in living epithelial tissues.

These challenges have motivated our work that is hosted in this paper. Hence, we present here, for the first time, results from the Global Sensitivity Analysis (GSA) of a

Manuscript received April 15, 2011. This research has been co-financed by the European Union (European Social Fund – ESF) and Greek national funds through the Operational Program "Education and Lifelong Learning" of the National Strategic Reference Framework (NSRF) - Research Funding Program: Heracleitus II. Investing in knowledge society through the European Social Fund.

C. Balas is with the Department of Electronic and Computer Engineering, Technical University of Crete, Chania 73100, Crete, Greece. (phone: +30-28210-37212; fax: +30-28210-37542; e-mail: balas@electronics.tuc.gr).

G. Papoutsoglou is with the Department of Electronic and Computer En-gineering, Technical University of Crete, Chania 73100, Greece (e-mail: gpap@electronics.tuc.gr).

A. Anastasopoulou is with the Department of Electronic and Computer En-gineering, Technical University of Crete, Chania 73100, Greece (e-mail: antigoni.a@gmail.com).

G. Stavrakakis is with the Department of Electronic and Computer Engineering, Technical University of Crete, Chania 73100, Crete, Greece. (e-mail: gstavr@elci.tuc.gr).

P. Soutter is with the Department of Gynaecological Oncology, Hammersmith Hospital, Imperial College, London W12 0HS, United Kingdom. (e-mail: p.soutter@imperial.ac.uk).

computational model that we have developed by formulating the bio-optical processes in neoplastic epithelium of the cervix.

## II. Materials and Methods

### A. Generation of bio-optical signals

Optical biomarkers or contrast agents employed in molecular imaging have the unique property of generating measurable dynamic optical signals when they interact with biomolecular targets and processes of diagnostic importance. In live cell or tissue imaging the dynamics of the target's optical activation is regulated by the uptake kinetics of the biomarker. This implies that the quantitative monitoring and modeling of the generated dynamic optical signal can be used for assessing the biomarker's uptake kinetics, which can, in turn, provide valuable information for both functional and structural characteristics and for the associated abnormalities. A basic prerequisite for achieving this is to establish a pharmacokinetic model that accounts for all tissue structural characteristics and also for all biomarker transport phenomena in the living tissue. The second step is to fit the experimental data with the model's output characteristics and estimate tissue structural and functional characteristics by attempting to solve the inverse problem. On such grounds, we have established a pharmacokinetic model that describes the epithelial metabolic and transport pathways that are followed by dilute AA solution when it is topically applied to epithelial tissue [12].

Generally speaking, the cells that inhabit tumorigenic areas are capable of maintaining their cytoplasmic pH normal, at the expense of extracellular acidosis. The elevated acidity of the extracellular space (ES) of neoplastic layers causes AA molecules to remain largely undissociated. As such, they can passively penetrate the cell membrane of the neoplastic cells, with high selectivity. At the same time, the pH of the intracellular space (IS) is almost neutral, which results in the subsequent disassociation of the AA to hydrogen ($H^+$) and acetate ($Ac^-$) ions. Excess $H^+$ ions provoke conformational changes in nuclear proteins, which, in turn, results in local variations of the index of refraction of the nucleus. These index variations are changing the scattering characteristics of the tissue, converting the epithelium from transparent to an opaque, highly scattering medium, thus generating the *in vivo* measurable dynamic optical signal. At the same time, and in order to disseminate the imposed ionic load, the cell dynamically employs several short and long-term mechanisms such as physicochemical buffering and active proton extrusion and the phenomenon is transiently reversed. In addition, and because the cervical epithelium is stratified, AA also diffuses along the tissue cross-section through the tight junctions. These processes are repeated in the underlying neoplastic epithelial layers, increasing the number of diffusely reflected photons. Finally, AA is gradually consumed or drained into the stroma and the tissue restores its original optical properties.

### B. Modeling of bio-optical processes

Epithelial tissues appear in either monolayer or multilayer cell formations that, from a structural perspective, tend to homogenize during neoplasia development. As such, and based on the previous analysis, the developed model partitions the dysplastic proportion of the cervical epithelium into a stack of abnormal cell layers, which is delimited by a reservoir layer from above i.e. a repository that supplies the biomarker. Each cell layer is assumed to be a duplex entity of independent, well-stirred and kinetically homogeneous compartments, namely: an extracellular (ES) and an intracellular (IS) one. Diffusion between compartments and layers is realized by the passive trans-membrane transport of AA molecules and ions and by their paracellular flux through the tight junctions, respectively. Naturally then, model equations were developed considering the diffusion fluxes of non-ionic and ionic species, through these pathways, down to concentration and potential gradients and according to the Fick's Law and the Goldman-Hodgkin-Katz constant field equation, respectively [13],[14]. These are:

$$\dot{C}_{IS}^{TA_i} = a^{-1}\left(J_m^{AA_i} + J_m^{Ac^-}\right), \tag{1}$$

$$\dot{C}_{IS}^{H_i^+} = -\ln 10^{C_{IS}^{H_i^+}}\left(a\beta_{IS}\right)^{-1}\left(q_{IS}^i J_m^{AA_i} - w_{IS}^i J_m^{Ac_i^-} - J_p^{H_i^+}\right), \tag{2}$$

$$\dot{C}_{ES}^{TA_i} = b^{-1}J_m^{AA_i} + b^{-1}J_m^{Ac_i^-} + a^{-1}KJ_T^{AA_i} + a^{-1}KJ_T^{Ac_i^-} \text{ and} \tag{3}$$

$$\dot{C}_{ES}^{H_i^+} = -\ln 10^{C_{ES}^{H_i^+}}\beta_{ES}^{-1}\Big[q_{ES}^i\left(b^{-1}J_m^{AA_i} + a^{-1}KJ_T^{AA_i}\right) - w_{ES}^i\left(b^{-1}J_m^{Ac_i^-} + a^{-1}KJ_T^{Ac_i^-}\right) + b^{-1}J_p^{H_i^+} + a^{-1}KJ_T^{H_i^+}\Big], \tag{4}$$

where $\dot{C}$ represents the concentration time derivative, TA denotes the total AA concentration in both ionized and unionized form, $i$ the $i^{th}$ neoplastic layer ($i$=1,2,...,N), $a$ and $b$ are the linear dimensions of the IS and of the ES, where cubic and rectangular compartment geometries have been assumed, $J_m$ and $J_p$ denote the passive and active transmembrane fluxes between the ES and IS, respectively, $\beta$ is the buffering power, $q$ and $w$ account for the AA's dynamic ionization constants, including its self-burning effect, $K$ is a parameter that expresses the geometrical dimensions (length) of the tight junctions and $J_T$ is the total paracellular flux that corresponds to the difference between the incoming and outgoing molecular fluxes between consecutive layers through the tight junctions. Here, we have to note that, for the reservoir layer (3) and (4) are abolished and for the last layer the outgoing paracellular flux is replaced by the $K_vC$ term, where $K_V$ is the kinetic rate at the tissue boundary between the epithelium and the stroma and $C$ denotes the concentration of TA or AA in the layer. A mixed-integer, nonlinear algorithm is created that is solved numerically using Matlab™, with the purpose of providing, as model's output the intracellular AA and $H^+$ concentrations vs. time functions in both the IS and the ES. Table I summarizes nominal values and value ranges of the variables that comprise the model's input.

TABLE I

| Parameter | Value | Unit | Reference |
|---|---|---|---|
| $a$ | 10-20 | μm | [16] |
| $b$ | 0.1-0.8 | μm | [16] |
| $K_V$ | $10^{-6}$-$10^{-7}$ | M/s | [19] |
| $\beta_{ES}$ | 10-30 | mM | [21] |
| $\beta_{IS}$ | 10-50 | mM | [22] |
| N | 1-12 | - | [16] |
| $pH_{ES}$ | 6-7 | - | [20] |
| $pH_{IS}$ | 7-7.4 | - | [20] |
| $K^{-1}$ | 0.01-1 | μm | [23] |

The biological parameter value ranges used as model inputs. These are functional and structural features which have been shown to change during neoplasia growth.

### C. Global Sensitivity Analysis

It has become evident from previous analysis that the temporal characteristics of the emitted scattering signal are determined by the $H^+$ concentration dynamics in the total IS of the entire epithelium. Going one step further, we reasonably expect that the normalized concentration versus time predictions of the model will fit the normalized experimental dynamic scattering signals. For this reason, we employed global sensitivity analysis (GSA) with the purpose of identifying those neoplasia-specific biological features that are key determinants of the dynamic optical signal's characteristics.

Generally, GSA requires no a priori knowledge of an input/output relationship and/or model additivity. With GSA the model's output uncertainty is apportioned, quantitatively, to the input parameter variations that are causing this uncertainty treating each input parameter as a random variable that follows a distribution from which data are randomly sampled. On such basis, variance-based methods provide robust statistical inferences in condensed format, by decomposing the output variance $V(\mathrm{Y})$ into terms of increasing dimensionality:

$$V(\mathrm{Y}) = \sum_{i=1}^{N} V_i + \sum_i \sum_j V_{ij} + \sum_i \sum_j \sum_k V_{ijk} + \ldots + V_{1,2,\ldots,\mathrm{k}}, \qquad (5)$$

where, given a $k$-dimensional input space, $V_{ij\ldots k}$ captures the output variance, due to a single factor or by interaction of multiple ones ($V_i = V(\mathrm{E}(\mathrm{Y}|\mathrm{X}_i)$, $V_{ij} = V(E(\mathrm{Y}|\mathrm{X}_i,\mathrm{X}_j)) - V_i - V_j$ and so on). A single index term ($V_\mathrm{i}$) designates the main effect of factor $\mathrm{X}_i$ to the output Y and the measure $S_i = V_i/V(\mathrm{Y})$ is called the first-order sensitivity effect of $\mathrm{X}_i$ on Y and defines, quantitatively, the contribution of the factor $\mathrm{X}_i$ to the output variance, alone. A sensitivity measure that accounts for the interaction between input factors is the total order sensitivity index. It sums up the overall influence of a factor $\mathrm{X_i}$ on the output variance: $S_{Ti} = S_i + S_{ij} + \ldots + S_{ij\ldots k}$, where $i < j < \ldots < k$. If small, it implies that the influence is nominal and, hence, ascertains which of the factors have no effect on the output variance.

We calculate the sensitivity indices by employing improved Sobol's method. The method considers the variances in (5) as multidimensional integrals and estimates the later using a quasi-Monte Carlo algorithm [15]. Calculations assume that the probability distributions of both discrete and continuous input parameters to be uniform. This quasi-Monte Carlo algorithm was implemented and executed to Mathwork's Matlab™ environment and thirty thousand parameter sets were used for estimating the first and total order sensitivity indices. Since the bio-optical processes under investigation are dynamic in nature, we have calculated these indices, for all model input variables, as a function of the time lapsed after the application of the biomarker. The median was used as a metric for the overall ranking of the input variables for the purpose of identifying the key biological factors determining the model's output and the line shapes of the dynamic optical signals.

### D. Experimental Data

The experimental data were used for a preliminary validation of the model and of GSA predictions. These data were obtained from the cervical epithelium of women referred to routine colposcopic examination. A video camera was attached to the colposcope, which is an instrument providing magnified view of the cervix. A set of images were taken in time sequence after the topical application of 3% AA dilute solution and for 4 minutes. One additional image was captured depicting the cervical tissue points from which biopsy samples were taken. The video stream was post-processed for image registration and for calculating the diffuse reflectance (DR) vs. time curves, at the points from where the biopsy was taken, using the green channel registered snapshots. This enabled the correlation of the dynamic DR (DDR) profiles, which depict the AA-provoked temporal changes in the back-scattering characteristics of the cervix, with the histological grading of cervical intraepithelial neoplasia (CIN). In total, 30 DDR curves were used in this study, corresponding to 10 CIN I (low grade) and 20 CIN II, III (high grade) cervical neoplasias (biopsy confirmed).

## III. Results and Discussion

Fig. 1 illustrates the first order (dark gray) and the total order (light gray) sensitivity index estimates in (first order) descending sequence for all model input parameters. Due to the dynamic nature of the bio-optical phenomena under analysis, the sensitivity indices have been found to be time-dependent. For this reason and for the purpose of obtaining an overall ranking of the model's output sensitivities to input variables, the vertical axis values refer to the median of the time-dependent sensitivity values. As it can be seen the parameters that are highly ranked are the number of neoplastic layers (N), the size of the ES ($b$) the $pH_{ES}$ and the intracellular buffering ($\beta_{IS}$). The total index values for parameters $pH_{IS}$, $a$, $\beta_{ES}$, $K$ and $K_V$ were found to be smaller than 6.5%, indicating a fairly negligible influence of these parameters to the model's output. Therefore, without significant losses in accuracy, they can be kept constant at around their nominal values. This finding indicates that the dimensionality of the problem can be reduced, facilitating

the estimation of the most important subset of parameters. Parameters N and *b* are structural parameters that are known to be very closely correlated with the neoplasia growth. Particularly, it has been established that the number of neoplastic layers and the extracellular space are increasing with the neoplasia growth [16]. In fact these are the key parameters onto which the routine histological grading of tissue biopsies is based and therefore their diagnostic value is high and well established. The diagnostic/predictive importance of the $pH_{ES}$ parameter has only recently been indentified and appreciated. According to the so-called "acid-mediated tumor invasion model", there is a strong link of the reduced $pH_{ES}$ with the ability of tumor cells to form invasive cancers [17]. Particularly, it has been shown experimentally that $H^+$ flow to peritumoral normal tissue provokes normal cell necrosis or apoptosis and extracellular matrix degradation. Tumor cells develop resistance to acid-induced toxicity during carcinogenesis, which permits them to invade the damaged normal tissue. Finally, the high ranking of the intracellular buffering power ($\beta_{IS}$) suggests its active role to the $H^+$ concentration dynamics. This is valid since the rapid physico-chemical processes that are lumped in this parameter are the cell's dominant suppressors of the acute increase in intracellular protons ($H^+$), during the AA tissue diffusion [18]. Both $pH_{ES}$ and $\beta_{IS}$ are functional parameters and cannot be accessed in dead tissue (biopsy) samples. The fact that these two functional parameters, together with the aforementioned structural ones, are the key determinants of measured/modeled dynamic optical characteristics indicate that they can be estimated concurrently and for every spatial point through non invasive optical measurements. This can be done, in principle, through the solution of the inverse problem, but this issue lies outside the scope of this study comprising a subject of our ongoing research.

Fig. 2 illustrates the total sensitivity values of the most influential parameters as a function of time. Fig. 3 illustrates the 30 DR vs. time experimental curves, 10 corresponding to CIN I (low grade) and 20 CIN II and III (high grade). It can be clearly seen, by comparing these two figures, that there is a different relative contribution of each parameter to the various time points of the DR vs time curves. The part until the first 20 s of these curves is mainly affected by the parameter $\beta_{IS}$ and to a lesser extent by the extracellular space (*b*). The number of neoplastic layers N seems to be the key determinant of the peak DR vs. time values. The same applies for the $pH_{ES}$ values but for the endpoint values of the experimental curves. From these observations we can conclude that the parameters in discussion are significantly entangled together in almost all the experimental data points and therefore the simple solution of estimating them from slopes or peak values of the experimental curves cannot be a reasonable choice. We are currently working on the separated calculation of these parameters using global optimization approaches. As a preliminary attempt to validate the findings of GSA we use the curves illustrated in

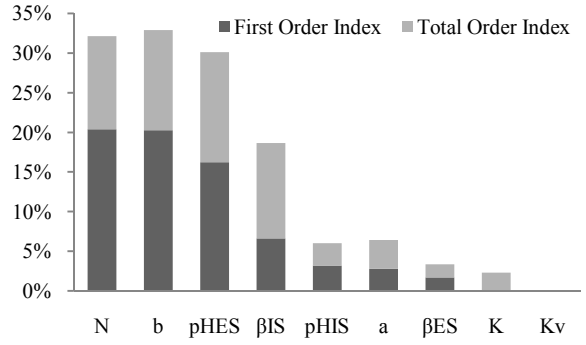


Fig. 1. The first order (dark gray) and the total order (light gray) sensitivity index estimates in (first order) descending sequence for all model input parameters The total sensitivity has been drawn together in order to depict the significance of parameter interactions to the output's uncertainty.

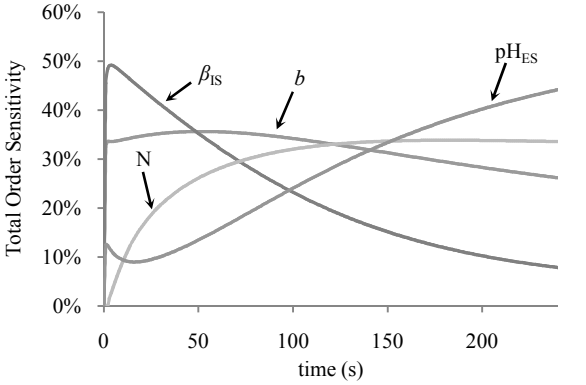


Fig. 2. The time dependence of the total sensitivity values of the model parameters that are the key determinants of the experimental data/model output characteristics.

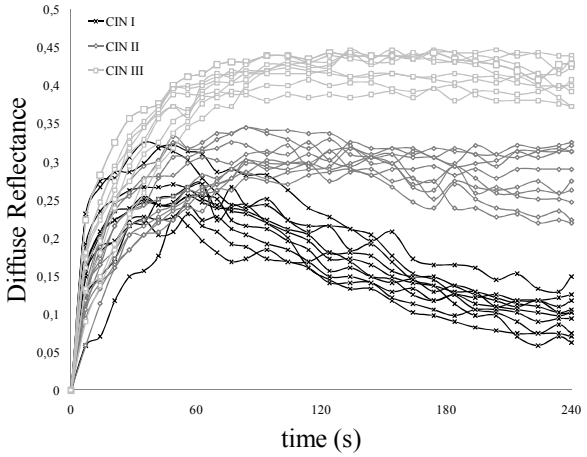


Fig. 3. Diffuse reflectance (DR) versus time experimental curves obtained from cervical tissues after the application of 3% acetic acid solution. Black curves correspond to CIN I lesions, dark gray to CIN II and light gray to CIN III.

fig. 2 and the information from [16], which correlates CIN grade and the number of neoplastic epithelial cell layers. The number of dysplastic layers are 1-4 for CIN I, 5-8 for CIN II and greater than 9 for CIN III. We validate GSA findings against N since this is the only parameter that can be assessed in a semi-quantitative manner in biopsy samples during routine histological analysis. At the time at which the N number total order sensitivity (142 s) peaks the median

DR for each CIN class is calculated. For the purpose of a rough estimation of the validity of GSA estimations, we consider a change from 1 to 10 in the number of layers (from CINI-CINIII) were we measure a 27% change in DR at t=142 s. This is a significant change within the range of values predicted by GSA. These findings suggest strongly that there is indeed a correspondence between theoretical predictions and experimental data.

## IV. Conclusion

We have combined *in vivo* dynamic imaging, *in silico* modeling and GSA for the detection and study of epithelial neoplasia. We have shown for the first time that the curve profiles of dynamic backscattering signals, that are measured *in vivo*, are mainly determined by two structural and two functional parameters. This finding implies that the dimensionality of the problem can be reduced remarkably, which facilitates the solution of the inverse problem: the concurrent estimation of all these parameters from *in vivo* measurements and for every spatial point. This achievement holds the promise to provide new insights in the study of epithelial neoplasia and novel non invasive diagnostic methods and devices, both contributing to cancer prevention.

## References


[1] H. A. Barton *et al.*, "Characterizing Uncertainty and Variability in Physiologically Based Pharmacokinetic Models: State of the Science and Needs for Research and Implementa-tion," *Toxicological Sciences,* vol. 99, no. 2, pp. 395-402, October 1, 2007.

[2] N. A. W. van Riel, "Dynamic modelling and analysis of biochemical networks: mechanism-based models and model-based experiments," *Briefings in Bioinformatics,* vol. 7, no. 4, pp. 364-374, December 1, 2006.

[3] P. Swietach *et al.*, "The role of carbonic anhydrase 9 in regulating extracellular and intracellular ph in three-dimensional tumor cell growths," *J Biol Chem,* vol. 284, no. 30, pp. 20299-310, Jul 24, 2009.

[4] W. Du, Y. Wang, Q. Luo and B.F. Liu, "Optical molecular imaging for systems biology: from molecule to organism," *Anal Bioanal Chem,* vol. 386, no. 3, pp. 444-57, Oct, 2006.

[5] C. Balas, "A novel optical imaging method for the early detection, quantitative grading, and mapping of cancerous and precancerous lesions of cervix," *IEEE Trans Biomed Eng,* vol. 48, no. 1, pp. 96-104, Jan, 2001.

[6] C. Balas, A. Dimoka, I. Orfanudaki, E. Koumantakis, "*In vivo* assessment of acetic acid–cervical tissue interaction using quantitative imaging of back-scattered light: its potential use for the *in vivo* cervical cancer detection grading and mapping," *SPIE-Optical Biopsies and Microscopic Techniques*, vol. 3568, pp. 31-37, 1999.

[7] C. Balas, and D. Pelecoudas, *System for characterization and mapping of tissue lesions*, U.S. Patent 7 515 952, April 7, 2009.

[8] C. Balas *et al.*, "*In vivo* detection and staging of epithelial dysplasias and malignancies based on the quantitative assessment of acetic acid-tissue interaction kinetics," *Journal of Photochemistry*, vol. 52, no. 1-3, pp. 153-157, 1999.

[9] I. M. Stefanaki *et al.*, "*In vivo* detection of human papilloma virus-induced lesions of anogenital area after application of acetic acid: a novel and accurate approach to a trivial method," *Journal of Photochemistry and Photobiology B-Biology,* vol. 65, no. 2-3, pp. 115-121, Dec. 31, 2001.

[10] J. Louwers *et al.*, "Dynamic spectral imaging colposcopy: higher sensitivity for detection of premalignant cervical lesions," *BJOG,* vol. 118, no. 3, pp. 309-18, Feb, 2011.

[11] W. P. Soutter *et al.*, "Dynamic spectral imaging: improving colposcopy," *Clin Cancer Res,* vol. 15, no. 5, pp. 1814-20, Mar. 1, 2009.

[12] C. Balas, G. Papoutsoglou, and A. Potirakis, "*In vivo* molecular imaging of cervical neoplasia using acetic acid as biomarker," *Ieee Journal of Selected Topics in Quantum Electronics,* vol. 14, no. 1, pp. 29-42, Jan-Feb, 2008.

[13] W. F. Boron, and P. DeWeer, "Intracellular pH transients in squid giant-axon caused by CO2, NH3 and metabolic inhibitors," *Journal of General Physiology,* vol. 67, no. 1, pp. 91-112, 1976.

[14] D. W. Keifer, and A. Roos, "Membrane-Permeability to the Molecular and Ionic Forms of Dmo in Barnacle Muscle," *American Journal of Physiology,* vol. 240, no. 1, pp. C73-C79, 1981.

[15] A. Saltelli *et al.*, "Variance based sensitivity analysis of model output. Design and estimator for the total sensitivity index," *Computer Physics Communications,* vol. 181, no. 2, pp. 259-270, Feb, 2010.

[16] D. C. Walker *et al.*, "A study of the morphological parameters of cervical squamous epithelium," *Physiological Measurements,* vol. 24 pp. 1–15, 2003.

[17] R. A. Gatenby, and E. T. Gawlinski, "The glycolytic phenotype in carcinogenesis and tumor invasion: insights through mathematical models," *Cancer Res,* vol. 63, no. 14, pp. 3847-54, Jul 15, 2003.

[18] W. F. Boron, and M. O. Bevensee, "Control of Intracellular pH," *Seldin and Giebisch's The kidney : physiology & pathophysiology*, R. J. Alpern and S. C. Hebert, eds., pp. 1429-1479, Amsterdam ; London: Academic, 2008.

[19] R. K. Jain,"Transport of molecules across tumor vasculature, " *Cancer and Metastasis Reviews*, vol. 6, pp. 559-593, 1986

[20] P. Swietach, R. D. Vaughan-Jones and A. L. Harris, "Regulation of tumor pH and the role of carbonic anhydrase 9," *Cancer Metastasis Reviews*, vol. 26, pp 299-310, 2007

[21] P.A. Schornack and R.J. Gillies, "Contributions of cell metabolism and H+ diffusion to the acidic pH of tumors," *Neoplasia*, vol. 5, no. 2, pp 135-145, 2003.

[22] M. J. Boyer, M. Barnard, D.W. Hedley and I.F. Tannock, "Regulation of intracellular pH in subpopulations of cells derived from spheroids and solid tumours," *British Journal of Cancer*, vol. 68, no. 5, pp 890-897, 1993.

[23] L. Langbein, *et al*., "Tight junctions and compositionally related junctional structures in mammalian stratified epithelia and cell cultures derived therefrom," *European Journal of Cell Biology*, vol. 81, pp. 419-435, 2002.